Signatures of superstrong magnetic fields in a limb solar flare from observations of the Hα line

Article *in* Advances in Space Research · April 2022

DOI: 10.1016/j.asr.2022.04.012

2 authors:

Ivan I Yakovkin
Taras Shevchenko National University of Kyiv
41 PUBLICATIONS **69** CITATIONS
SEE PROFILE

Vsevolod G. Lozitsky
Taras Shevchenko National University of Kyiv
177 PUBLICATIONS **673** CITATIONS
SEE PROFILE

https://doi.org/10.1016/j.asr.2022.04.012

Signatures of superstrong magnetic fields in a limb solar flare from observations of the Hα line

I.I. Yakovkin, V.G. Lozitsky*

Astronomical Observatory of the Taras Shevchenko National University of Kyiv, Observatorna St. 3, Kyiv 04053, Ukraine

Received 2022 February 12

Abstract

We present signatures of the super-strong magnetic fields of almost 10^5 Gauss range in the limb solar flare of 14 July 2005 at the altitudes of 5 – 30 Mm during the post-peak phase of the flare. These features follow from the study of the Stokes *V* profile in the Hα line at large distances of 1.5 up to 4 Å from its center. A reliable circular polarization (till 1%) was found that changes its sign when crossing the line center. The profile of the polarization differs significantly from the intensity gradient profile dI/dλ, which indicates the strong magnetic field mode. If these features are interpreted as manifestations of the Zeeman effect, the corresponding magnetic field strength reaches ~ 90 kG. Similar spectral manifestations were not found in another bright emission formation on the solar limb, namely in the active prominence of 24 July 1999. Theoretical analysis of the picture of the Zeeman effect for the case of such giant fields shows that the σ components of the Hα line should be quite narrow (~ 0.2 Å) due to the Pashen-Back effect, despite the complex picture of the splitting of this line. Since the observed widths of the peaks of the Stokes *V* profiles are much wider, this may mean a certain dispersion of the magnetic field strengths in the flare, at which the maximum strengths can be even some greater than those indicated above.

Keywords: Sun, solar activity, limb solar flare, line profiles, magnetic fields, strengths of 10^5 range.

1. Introduction

The possible existence of superstrong magnetic fields (> 10^3 G) in solar flares was supposed for the first time, likely, by Bruce (1966). He supposed that long wings of the Hα line in flares (up to 8 Å) could arise due to the Zeeman effect in 10–100 kG fields. In fact, this is one of several possible interpretations, which explain the line-profile broadening accounting also for turbulent velocities, temperature, and electric fields. To distinguish these effects, the full Stokes parameters *I, Q, U,* and *V* of polarized light are needed.

*Corresponding author. Address: Astronomical Observatory of Taras Shevchenko National University of Kyiv, 3, Observatorna str., Kyiv 04053, Ukraine.
Tel.: +380 44 486 0906; fax: +380 44 481 4478.
E-mail addresses: yakovkinii@gmail.com (Yakovkin I.I.), lozitsky_v@ukr.net (Lozitsky V.G.).

On the other hand, if the magnetic field is subtelescopically tangled (for instance, in form of mixed polarity structures) the Stokes diagnostics could become useless: we can have an essential broadening of Stokes *I* profile but practically zero polarization on different distances from line center.

As far as we know, till present, no special attempts have been made to search for manifestations of the Zeeman effect from extremely strong fields localized in the distant wings of the Hα line (≥ 1.5 Å from line center). The most important indications in favor of such fields were obtained from other spectral lines, in particular, from lines with very small Landé factors (Lozitsky, 1993, 1998, 2011, 2015; Lozitsky & Staude, 2008). In particular, it was shown that Stokes $I \pm V$ profiles of some such lines in flares, e.g. Fe I $^5F_1{}^5F_1$ λ = 5123.723 Å and Fe I $^5F_1{}^5D_0$ λ = 5434.527 Å, sometimes have narrow split emission peaks in their cores. Both spectral lines have zero theoretical Lande factors for the case of LS coupling, but their empirical Lande factors, determined in the laboratory, strictly speaking, are not zero and equal to –0.013 and –0.014, respectively (Zemanek & Stefanov,1976; Landi Degl'Innocenti, 1982). Measured splitting of emission peaks in cores of $I \pm V$ profiles was observed to be significant, reaching 36 mÅ, whereas similar splitting in $I \pm Q$ profiles was found to be close to zero (≤ 5 mÅ). Taking into account that non-flare profiles did not display similar effects, it was assumed to be the Zeeman effect manifestation of the superstrong magnetic fields reaching 90–100 kG.

Possible indications of even stronger fields of ~10^5 G range were found outside the core of the Fe I 5434.5 line, at its wings. In a solar flare, $I \pm V$ profiles of this line had local extrema of bisector splitting localized at distances of 0.13–0.18 Å from line center (Lozitsky, 2009). Such peculiarities could arise in a two-component magnetic field, with weak and strong components. In this case, we should observe the superposition of line profiles from two magnetic field modes, and the specified extrema can reflect the true position (i.e. Zeeman splitting) of the sigma components from strong field mode localized in spatially unresolved structures. Taking into account that probable instrumental effects were about 3–5 times less than observed amplitudes of the mentioned extrema, the presence of local magnetic fields of 0.7–0.9 MG was supposed.

These results refer to the "upper photosphere – minimum temperature zone" altitude range; about 0.4-0.6 Mm above the level $\tau_5 = 1$. Of course, it is interesting to check whether there are similar indications for high altitudes, which correspond to the chromosphere and to the lower corona. In view of the strong rarefaction of matter in the chromosphere and corona, one can hope to record the corresponding contrasting spectral effects only in limb solar flares. Lately, on a base of magnetic field measurements in a limb solar flare by hydrogen, helium, and ionized calcium lines it was found that very strong kG magnetic fields (up to about 3 kG) existed at the heights of 10–18 Mm above the level of the photosphere (Yakovkin et al., 2021). However, this work did not study in detail the distant wings of spectral lines, which could contain signatures of even stronger fields.

Other authors also obtained similar results for the lower corona. The first measurements of this kind were made by Koval (1977) using the Hα line. It was found that the magnitude of the magnetic field, measured by the relative splitting of the line in orthogonal circular polarizations (i.e., in the $I + V$ and $I - V$ spectra, where *I* and *V* are the corresponding Stokes parameters), is typically several hundred gauss. However, a case of a rather significant relative displacement of the $I \pm V$ profiles corresponding to a magnetic field strength of 9 kG was also detected (Koval, 1977). Koval (1977)

had the following point of view: "However, such large values are unlikely in the light of existing ideas about the structure of magnetic fields in the solar atmosphere".

Similar strong magnetic fields were measured also in the X1.2 class limb flare that occurred on 2005 July 14 (Lozitsky & Statsenko, 2006). The obtained results relate mainly to the lower solar corona and correspond to heights of 2–10 Mm above the level of the photosphere. From the measurements of the $I \pm V$ profiles splitting in the Hα line by the "center of gravity" method, it was concluded that magnetic fields of B = 200–300 G existed at the indicated heights. However, a detailed study of the bisectors of the $I \pm V$ profiles showed that the magnetic field in the flare volume was significantly heterogeneous, which is evident from the fact that the bisectors of the $I \pm V$ profiles were non-parallel. In particular, a local peak of bisector splitting was detected at a considerable distance $\Delta\lambda$ from the line core, $\Delta\lambda \approx 1.1$ Å. If this peak of bisector splitting is assumed to reflect the regime of a strong magnetic field and correspond to the true localization of weak Zeeman sigma components, the corresponding magnetic field is ≈ 50 kG.

Magnetic fields of 200 G were measured using the Hα line also in the M7.7 limb flare on 2012 July 19 (Kirichek et al., 2013). The results obtained refer to a rather high altitude above the limb, about 40 Mm. In this case, a significant lack of parallelism of the bisectors of the $I \pm V$ profiles was observed too, with a maximum of their splitting at a distance of 0.4 Å from the center of the emission profile. In the mentioned study, a theoretical MHD force-free model was proposed that allows to explain the existence of such strong fields in the corona due to the strong twisting of the field lines. According to numerical estimations in the frame of the model, the magnetic field strength increases by about 2 orders in comparison with the weak external field of 1–2 G typical for the solar corona.

Kuridze et al. (2019) reported on unique observations of flaring coronal loops above the solar limb using the high-resolution imaging spectropolarimetry in the Ca II 8542 Å line from the Swedish 1m Solar Telescope. The authors found magnetic field strengths as high as 350 G at heights up to 25 Mm above the solar limb. This value is similar to the result by Kirichek et al (2013). Microwave and hard X-ray observations of the X8.2 solar limb flare on 2017 September 10 revealed regions of high magnetic field strength (up to 520 G) at projected heights of about 25 Mm (Gary et al., 2018). Kleint (2017) studied chromospheric line-of-sight magnetic field B_{LOS} changes based on spectropolarimetry of the Ca II 8542 Å line obtained with the DST/IBIS instrument during an X1 flare on the solar disk. It was shown that these changes are stronger (< 640 Mx cm^{-2}) and appear in larger areas than their photospheric counterparts (< 320 Mx cm^{-2}). However, these measurements are difficult to compare with the results discussed above for limb flares, since they relate to significantly lower heights in the atmosphere.

Libbrecht et al. (2019) found magnetic field strengths of 2500 G in a C3.6-class flare, based on the first SST/CRISP spectro-polarimetric observations in the He I D3 line. A record-breaking coronal magnetic field strength of about 4000 G in solar active region 12673 was found by Anfinogentov et al. (2019) using microwave observations. Combining the photospheric vector measurements of the magnetic field and the coronal probing, a nonlinear force-free field coronal model was created, which presents the highest coronal magnetic field strengths reported at various coronal heights.

At present, the variation of the vector magnetic field along structures in the solar corona remains unmeasured. An important step in this direction was made by Schad et al. (2016) using

spectropolarimetric data of the He I 10830 Å triplet obtained at the Dunn Solar Telescope with the Facility Infrared Spectropolarimeter. Spectropolarimetric inversions indicate that the magnetic field is generally oriented along the coronal loop axis. Multi-wavelength observations of polarized radio emission in the microwave range also give evidence of strong magnetic fields (up to 1800 G) in the low solar corona above active regions, outside flaring times (Bogod et al., 2012). Magnetic fields in range a few hundred gauss were measured in solar filaments by Kuckein et al. (2009, 2020) using same HeI line. The vector magnetic field till 600-800 G was measured simultaneously in the photosphere and upper chromosphere from spectro-polarimetric scans made in the Si I 1082.7 nm and He I 1083.0 nm line of an active region filament (Xu et al., 2012).

Fleishman et al. (2020) presented microwave observations of the X8.2 limb flare on 2017 September 10, demonstrating spatial and temporal changes in the coronal magnetic field. The authors found that for 2 minutes during the flare, the field decays at a rate of about 5 Gauss per second, as measured within a flare subvolume of ~10^{28} cm^3. This fast rate of decay implies a sufficiently strong electric field to account for the particle acceleration that produces the microwave emission. The decrease in the stored magnetic energy is enough to power the solar flare, including the associated eruption, particle acceleration, and plasma heating. Chen et al. (2020) studied for the same event the coronal magnetic field and the relativistic electrons along the flare current sheet. The measured magnetic field profile reveals a local maximum where the reconnecting field lines of opposite polarities closely approach each other, indicative of the reconnection X-point. A strong reconnection electric field of about 4,000 V m^{-1} is inferred near the X-point.

Yadav R. et al (2020) presented high-resolution and multi-line observations of a C2-class solar flare that occurred in NOAA AR 12740 on May 6, 2019. The rise, peak, and decay phases of the flare were recorded continuously and quasi-simultaneously in the Ca II K line with the CHROMIS instrument, the Ca II 8542 Å and Fe I 6173 Å lines with the CRISP instrument at the SST. The temporal analysis of the LOS magnetic field at the flare points exhibits a maximum change of ~600 G. After the flare, the LOS magnetic field decreases to the non-flaring value, exhibiting no permanent or step-wise change.

A broad comparison of the results of different authors and methods is presented in the paper by Sasikumar Raja et al. (2022). The authors note that the magnitude of the recorded magnetic field as whole increases from ~1 G at 2 solar radii to more than 3 kG at 10-20 Mm. Magnetic fields in the range of 600-1400 G were also found by Wei Yudian et al (2021) in the partially erupting filament in a solar flare.

In the present paper, we analyze the fine spectral effects in the Hα line, taking into account the theoretical aspects of its complex Zeeman splitting in the case of especially strong magnetic fields. The specific purpose of our analysis is to test Bruce's (1966) hypothesis about the possible existence of superstrong magnetic fields in the solar flare, which reach ~100 kG.

2. Observations and data processing

We analyze the observational material that relates to the limb solar flare of July 14, 2005. This flare of the X1.2 class occurred at 10:16 UT in the NOOA 10786 group at 11N and 90W coordinates, reaching the peak phase at 10:55 UT. The flare was observed by Lozitsky V.G.,

Lozitska N.I., and Statsenko M.M. on the Echelle spectrograph of the horizontal solar telescope of the Astronomical Observatory of Taras Shevchenko National University of Kiev (Lozitsky, 2016). The main value of observations with the Echelle spectrograph is that a wide spectrum interval, from 3800 to 6600 Å, can be recorded simultaneously where many thousands of spectral lines can be observed. Another advantage of such observations is that I +V and I – V spectra were obtained simultaneously, on separate adjacent bands of the spectrograms. This was made thanks to the fact that the circular polarization analyzer consisted of a λ/4 plate in front of the entrance slit of the spectrograph and a beam splitting prism (analogous to the Wollaston prism) behind the entrance slit. Therefore, $I + V$ and $I – V$ spectra relate to the same moment of time and to the same locations on the Sun.

Echelle Zeeman-spectrograms of the flare were obtained at 11:51, 12:02, 12:07, and 12:10 UT using the ORWO WP3 photo-plates. The mentioned article by Lozitsky and Statsenko (2006) is dedicated to the analyses of the 12:07 moment of this flare and it presents the indications of super-strong magnetic fields of up to 50 kG in magnitude. It is interesting and important to verify whether there are similar indications in other moments of the flare. That is why we analyze below in details the 12:10 UT moment, which is close in time to the 12:07 UT, i.e. 75 minutes after the peak of the flare. For comparison, we also analyze the data related to the active prominence of July 24, 1999, for time 6:49 UT. The exposures of all of the spectra were 60 seconds.

Since we planned to search for very fine peculiarities in distant wings of spectral lines and in the adjacent continuum, it was advisable to analyze only the most intense emissions that provided the highest signal-to-noise ratio. As it turned out, only the Hα line had such a property on our spectral material; that is why in this paper we are limited to the Hα line and do not analyze possible subtle spectral effects in other lines.

As can be seen from the Figure 1, the photosphere did not hit the entrance slit of the spectrograph during the observations of the flare, while this happened during the observations of the prominence, which made it possible to reliably link the data to the altitude scale in the solar atmosphere. For the flare, we can only indicate approximate heights, based on sketches of the edge of the solar disk relative to the entrance slit of the spectrograph. The flare heights indicated below represent the lower limit of the actual heights, and the actual heights may be about 5 Mm higher than those pointed out in comments for Figs. 2-5 below.

From Figure 1 it follows that the spectrum of the flare looks more modest and with less broadening of the Hα line than the spectrum of the active prominence. Nevertheless, as will be shown below, it was in the flare that the signatures of especially powerful magnetic fields were detected.

The spectrograms were scanned using an Epson Perfection V 550 scanner, which allows to obtain two-dimensional scans of images recorded on transparent films or on photo-plates. In order to convert the density into intensity, it is necessary to take into account the characteristic curve of the photographic material as well as the curve of the scanner itself. Both curves are nonlinear and require preliminary determination by special methods. In order to do this, we used a step attenuator, for which transmittances are precisely known. When converting photometrical densities into intensities, the scattered light in the spectrograph was taken into account by subtracting the intensities corresponding to the intervals between images of different orders of the spectrum of the Echelle spectrograph.

During the pre-processing of observational data, spectrum recordings of $I + V$ and $I – V$ profiles in intensities were mutually linked by wavelengths using narrow telluric lines; the accuracy of this binding is about 1-2 mÅ. The next step in data processing was to find the normalized intensities, i.e. local intensities, expressed in units of maximum intensity in the central part of the H-alpha line profile. Since the absolute intensities of the I + V and I - V spectra differed insignificantly, by about ~ 10% (which is partially seen from Fig. 1), this normalization led to the fact that the intensities of both spectra leveled off in the central part of the H-alpha, but almost did not change in the distant wings. After these two steps, the I and V profiles were calculated using $I + V$ and $I – V$ profiles.

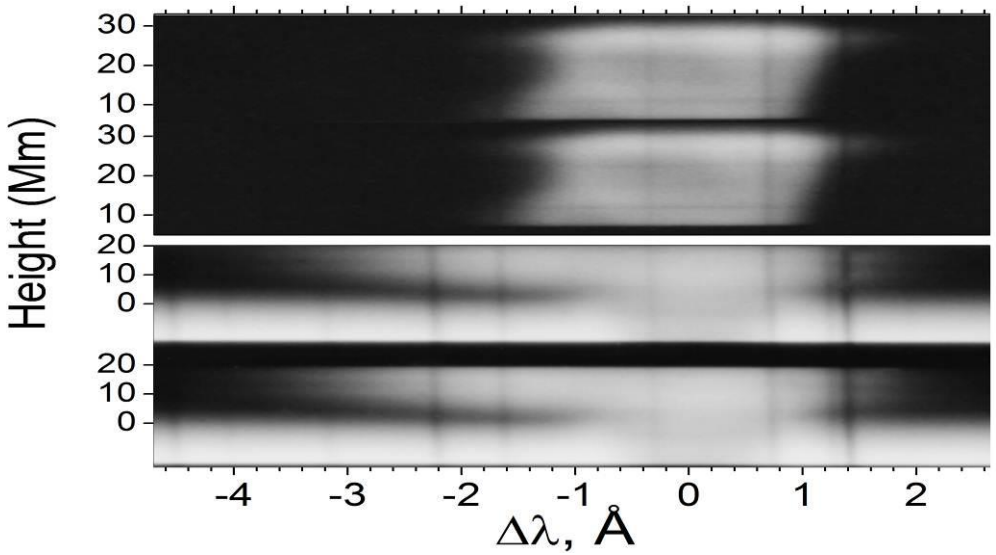

Fig. 1. Fragments of the Zeeman spectrograms which present the Hα line in limb solar flare of July 14, 2005 (top) and active prominence July 24, 1999 (bottom). The top and bottom half of spectrograms correspond to the $I – V$ and $I + V$ spectra, respectively. The zero-point on the abscissa corresponds to the center of the Fraunhofer profile.

Although in the case of the Hα line the basic information about the magnetic field is contained in the V profile, the I profiles are also important as a tool for determining the weak field regime. At really weak magnetic splitting $\Delta\lambda_H$, when it is much smaller than the Doppler width of the spectral line $\Delta\lambda_D$, the observed V profile should be similar to the intensity gradient profile $dI/d\lambda$ (Unno, 1956).

However, this relation is only valid for smooth Gaussian profiles; if the line profiles are not Gaussian but have, for example, a truncated vertex of the such as shown below on Fig. 2, the relation $\Delta\lambda_V < \Delta\lambda_I$ may also indicate the deviation from the weak field regime.

3. Effective magnetic field B_{eff}

By the effective magnetic field B_{eff} we mean the magnetic field corresponding to the weak-field approximation and the one-component model. It can be measured by the displacement of the

"centers of gravity" of the $I + V$ profiles relative to the $I - V$ profiles, or by the splitting of the bisectors of these profiles. Of course, in such measurements, areas of strong blending of the Hα line with telluric lines should be excluded from consideration. Physically, such a magnetic field is closest to the longitudinal component B_{LOS} of the strength vector, but under the assumption that the filling factor f is equal to unity. If in fact $f < 1$, then the actual value of the local fields can be estimated as B_{eff} / f.

Fig. 1 suggests that at the optimal alignment of telluric lines, the I + V and I-V profiles of the H-alpha line do not have a significant relative shift, if we consider only areas within ± 1.5 Å from the "center of gravity" of intense emission. However, a detailed inspection shows that in fact a relative shift does exist and is different in different places of the solar flare. According to the measurements, the average absolute field B_{eff} value is 400 G in the height range of 5-30 Mm with typical measurement errors of 100 G. The strongest magnetic fields of -1250 G and +1000 G were recorded at altitudes of 13-14 Mm and 29-30 Mm, respectively. In principle, these are quite strong magnetic fields for heights of the lower solar corona, where the plasma concentration is very low. It should be noted that much stronger magnetic fields (up to 3 kG) were measured by the same method in another limb solar flare, 1981 July 17 (Yakovkin and Lozitsky, 2021).

4. Stokes *V* profiles in the flare

In order to detect subtle spectral effects in the Hα line profiles, we averaged the data over significant spatial intervals, starting with 1 Mm of the flare height, see Fig. 2. This Figure shows the I ± V profiles of the Hα together with telluric lines for the photometric sections Nos. 13 and 15, which corresponds to the heights 19-20 and 17-18 Mm. In this Figure, the arrows show the places in the far wings of the $I \pm V$ profiles, in which there is a noticeable circular polarization, which changes its sign when passing through the center of the Hα line. This can be seen from the fact that in the "blue" wing of the line, at a distance from the center $\Delta\lambda \approx -1800$ mÅ, the profile $I + V$ (shown by a solid curve) is generally higher than the profile $I - V$, shown by the dotted curve. In the "red" wing of the line, at the same distances from the center, the situation is reversed – the $I + V$ profile is generally lower than the $I - V$ profile. That is, the Stokes V changes its sign when passing through the center of the line, as it should be in the Zeeman effect. From Fig. 2 it follows that these features are well repeated for two adjacent flare points, each of which has a total length of 1 Mm.

If the averaging interval is extended by the height in the atmosphere and by the wavelengths in the spectrum, the main features of the parameter V are as follows (Figs. 3 and 4). First, the reliability of the change in the sign of polarization is confirmed when passing through the line center. In these Figures, vertical intervals represent the root mean square errors of the mean value of the V parameter. The profile of parameter $dI/d\lambda$ is also given for comparison. Secondly, the picture of the parameter V remains more or less symmetrical about the center of the line, but only at a not too large averaging interval, up to 5 Mm (Fig. 3). If the interval is further expanded to 14 Mm, then there are some new subtle details that are not repeated fully in the transition from "blue" to "red" wings of the line (Fig. 4). Still, in both cases (for 5 Mm and for 14 Mm), we see the

preservation of two effects: (a) a change in sign when passing through the center of the line and (b) a reliable maximum of polarization at distances $\Delta\lambda \approx \pm$ (1.8-1.9) Å.

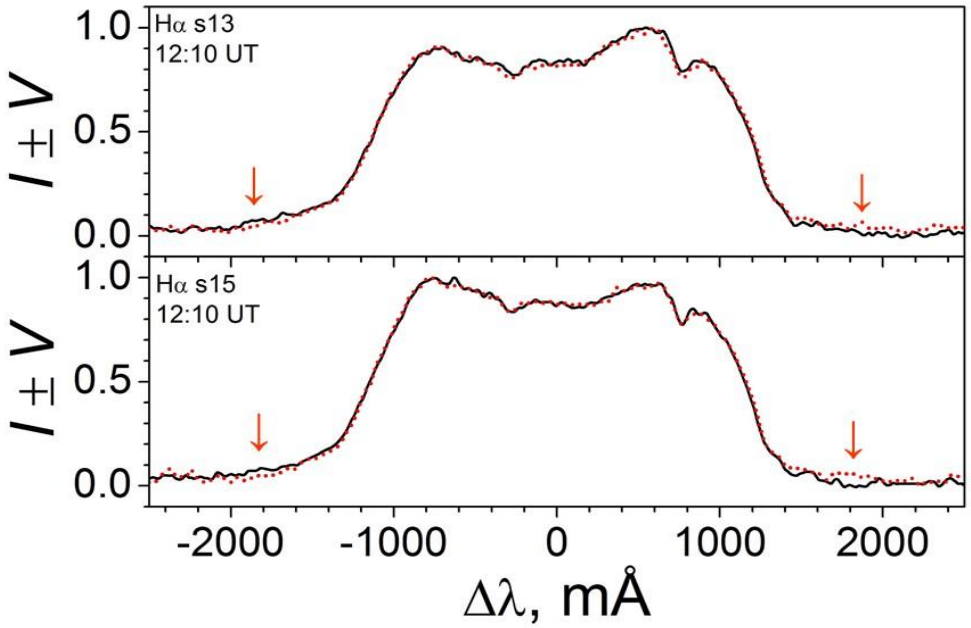

Fig. 2. Comparison of $I \pm V$ profiles of Hα line for two adjacent photometric sections with a width of 1 Mm each, which correspond to the heights 19-20 and 17-18 Mm.

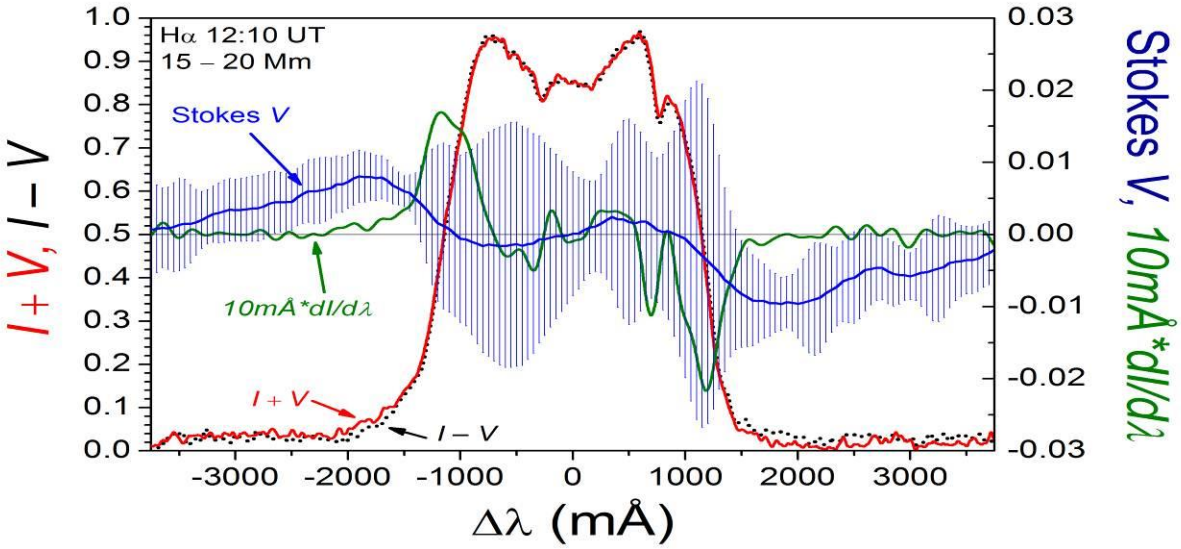

Fig. 3. Comparison of the observed $I \pm V$, V, and dI/dλ profiles for the Hα line in the solar flare of July 14, 2005, at an averaging interval of 15-20 Mm (see the text).

From Figs. 3 and 4 it follows that the dI/dλ profile has two clear peaks of opposite sign, which are located at a distance $\Delta\lambda \approx \pm$ 1.2 Å from the center. There is also another narrow peak of the dI/dλ parameter at the distance $\Delta\lambda \approx +$ 0.66 Å from the emission center, but it is related to the

telluric line. Following from the shape of the d*I*/dλ parameter profile, we should not expect significant circular polarization at distances Δλ ≥ 1.5 Å for the case of a weak field mode. Meanwhile, Figs. 3-4 show that such polarization does exist in some places, and it reaches ≈ 1%, significantly exceeding the measurement errors. As it was pointed above, the places of significant polarization are located at middle distance of Δλ ≈ ± (1.8-1.9) Å (Figs. 3-4), and it is almost symmetrical with respect to the center of intense emission. It should be noted that the obvious signs of the Zeeman effect are a sign-variable circular polarization and its symmetrical pattern relative to the center of the line. However, this is only the case when the magnetic field has one component and there are no significant Doppler shifts caused by large radial velocities in the flare. It is possible that the clear difference between the Stokes *V* in the "blue" and "red" wings of the line (Fig. 4) is caused precisely by the presence of several magnetic field components with different strengths and also by some Doppler shifts.

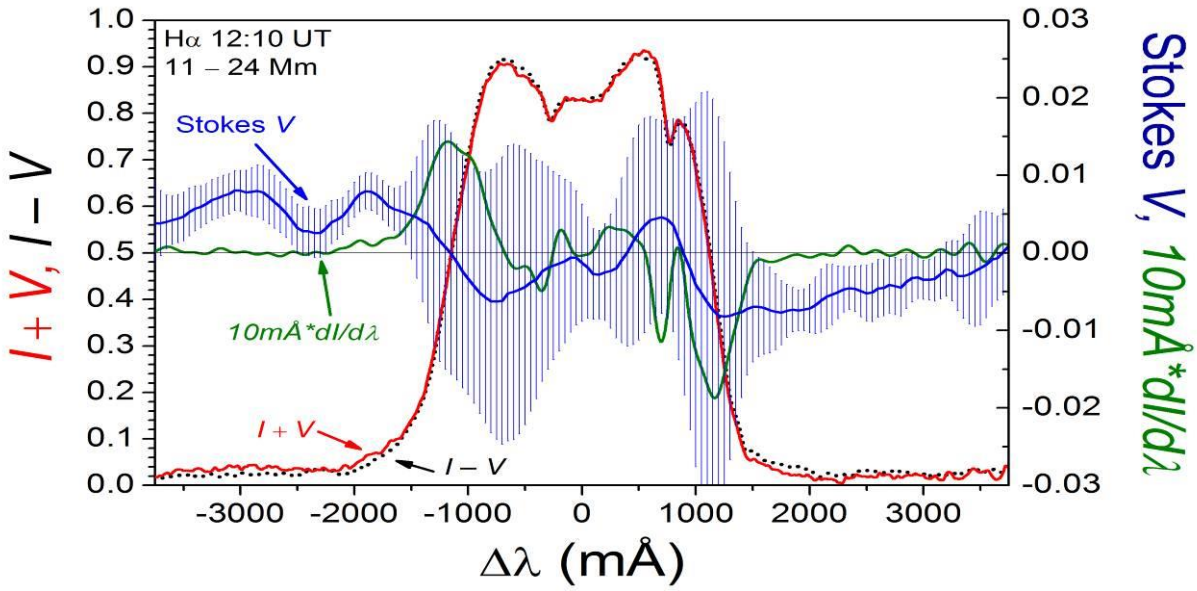

Fig. 4. The same as in Fig. 3, but for the heights of 11-24 Mm.

If this is indeed the case, then from an examination of Fig. 4 it follows that the corresponding Zeeman σ components should be quite narrow - much narrower than the intense line profile concentrated in the range ± 1.5 Å. This requires separate consideration of whether such a narrow detail is theoretically possible under the Zeeman effect in the Hα line, given its very complex (non-triplet) structure. This issue is discussed in detail below in Section 6.

5. Stokes *V* profiles in the prominence

The active prominence of July 24, 1999, was selected for comparison as a similar object to the specified solar flare, given its late (post-maximum) phase of development. It is known that limb

solar flares in the final stage of their evolution are quite similar to active prominences on the limb of the Sun.

Figures 5 and 6 show that in this prominence the emission in Stokes *V* is more asymmetric, as a result of which the "blue" peak of the d*I*/dλ parameter is more blurred and, moreover, it is blended by telluric lines.

However, the Stokes *V* profile is of the greatest interest here: it can be seen from both Figures that in different places of the prominence this profile does not have a reliable change of sign with respect to the emission center. That is, there are no indications of the Zeeman effect at distances Δλ = ± (1.5÷3.5) Å, as was found for the limb flare.

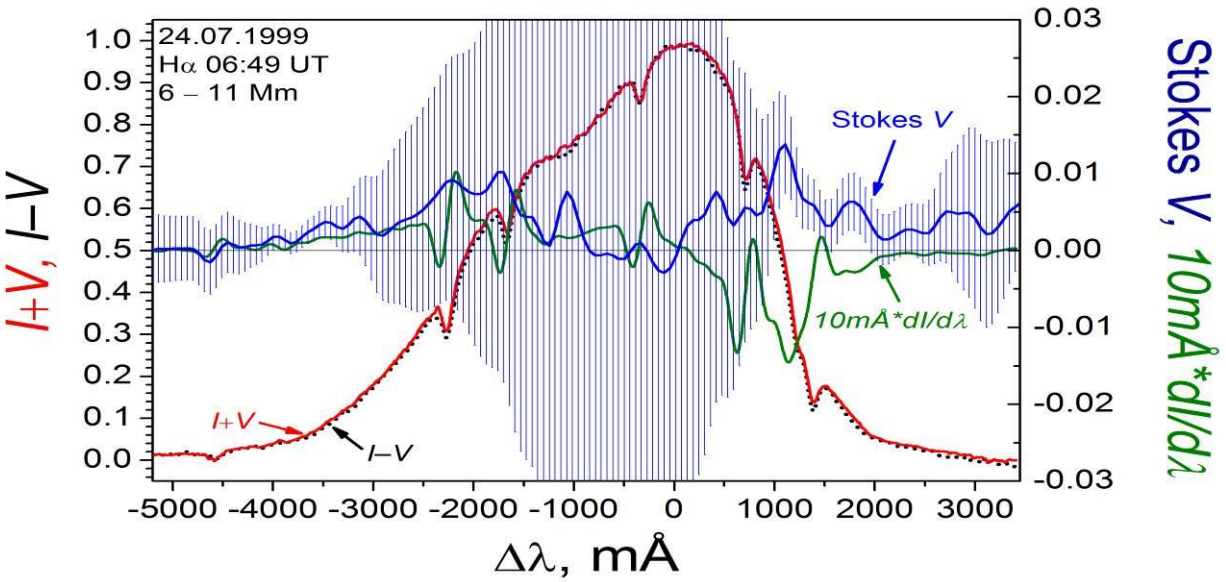

Fig. 5. The same as in Figs. 3-5, but for the active prominence of July 24, 1999. The presented data are the result of averaging by photometric sections 19, 21, and 23, which correspond to the heights of 6-11Mm.

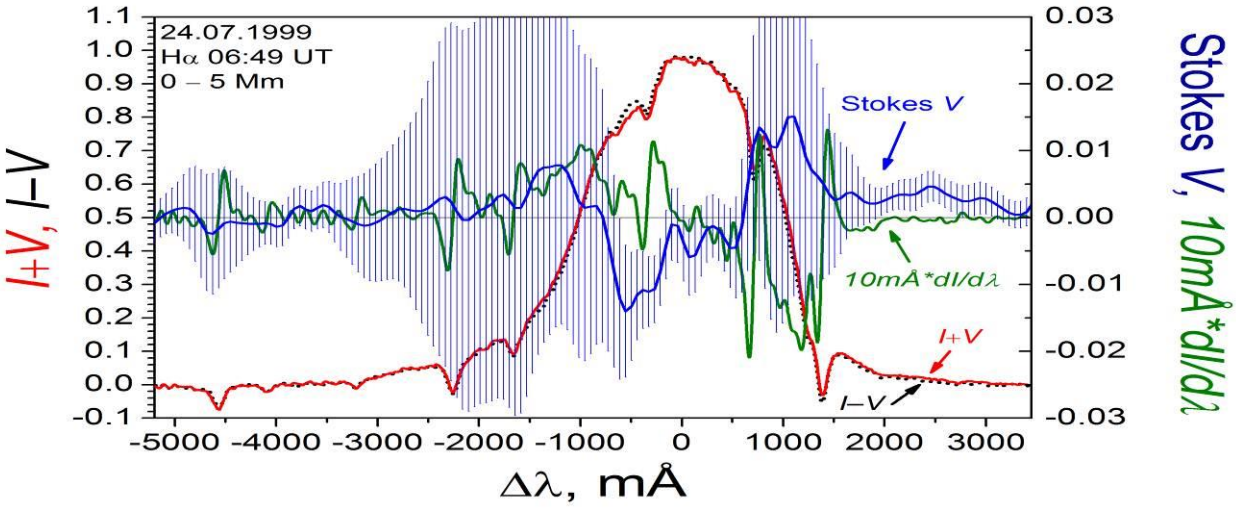

Fig. 6. The same as in Fig. 5, but for photometric sections 13, 15, and 17, which correspond to the heights of 0-5 Mm.

Therefore, the above analysis confirms the uniqueness of the observational material of the solar flare of July 14, 2005, first represented in the work of Lozitsky and Statsenko (2006). Although in the mentioned work there was a clear deviation from the weak field regime at a distance of $\Delta\lambda = \pm 1.1$ Å from the emission center in the H-alpha line, in this study we find a similar case at significantly larger distances $\Delta\lambda \approx \pm 2$ Å, which may indicate even stronger magnetic fields. But in order to properly substantiate this conclusion, we must consider in detail the theoretical aspects of the Zeeman effect in the H-alpha line under such giant magnetic fields.

6. Theoretical line profiles for the case of superstrong magnetic fields

Despite the simplicity of the Hydrogen atom, its spectral lines have a complex structure. Detailed studies (Kramida, 2010) show that it is appropriate to use different methods for different accuracy goals when describing the hydrogen spectrum.

In the most basic case, it suffices to solve the Schrödinger equation. This approach allows to obtain a basic structure of the hydrogen spectrum. Next, we can introduce the spin quantum number, which allows one to approximate the behavior of an atom in strong electric and magnetic fields. To describe the case of weaker fields, when the magnetic splitting of the spectral lines is smaller, one needs to take into account the fine structure of atomic levels. To do this, we have to solve the Pauli equation for the hydrogen atom. For even more precise solutions, one may use the Dirac equation and quantum electrodynamics.

Due to the high typical temperatures in the flare and the magnitude of the studied magnetic fields, the effects of the hyperfine structure must have a negligibly small effect on the shape of observed spectral line profiles. Therefore we have used the corresponding Pauli equation for the theoretical calculation of the H-alpha line profiles in a magnetic field (Blom,2005).

The calculation of the spectral line splitting due to magnetic field is often performed in one of the following approximations. The weak magnetic field approximation (WFA) – is used when the expected splitting of the lines is much smaller than the splitting of the fine structure. In this case, the Pauli equation without the magnetic field is solved exactly, and then the latter is taken into account using the perturbation theory. The opposite approximation of the strong magnetic fields is valid when the magnetic splitting of spectral lines is much larger than the fine structure splitting. This case corresponds to the full Paschen-Back effect, and the energies are calculated by analytically solving the Pauli equation in a magnetic field with no fine structure, and then accounting for the latter using perturbation techniques. However, both mentioned approaches are applicable for significantly limited ranges of magnetic fields.

It should be noted that this understanding of the modes of strong and weak magnetic fields in physics differs from that used in solar magnetometry. We recall that in the latter case, the weak-field regime means the case when the Zeeman splitting is much smaller than the observed spectral line width. In the same case, the strong field regime is understood as the case when the Zeeman splitting exceeds the width of the spectral magnetosensitive line.

During active processes on the Sun, the typical magnetic fields reach the order of several kilogauss in magnitude. In such a case, the corresponding Zeeman splittings are comparable to those of the fine structure. This means that for a correct calculation of the Zeeman effect in the H-

alpha line for these typical values of the magnitude of the magnetic fields we need to make a more general calculation. In this work, we calculated the Zeeman effect for the H-alpha line for arbitrary values of magnetic fields. For this purpose, both the interaction with the magnetic field and the spin-orbit interaction were considered as perturbations. This approach allows for a correct description of the shape and splitting of spectral lines at any values of magnetic fields, including the extreme cases of weak and strong fields.

The Hamiltonian for the electron in a hydrogen atom can be represented in the following form:

$$H = H_0 + H_{LS} + H_B + H_{rel} + H_{Darwin}. \quad (1)$$

The general shape of the Hamiltonian suggests the following steps in the theoretical calculations of the Zeeman effect for arbitrary values of the magnetic field (Bethe and Salpeter, 1957):

1. Obtain a solution for a hydrogen atom in the absence of magnetic fields without taking into account the spin-orbit interaction and relativistic corrections (H_0).
2. Assuming that the spin-orbit interaction (H_{LS}) and the interaction with the magnetic field (H_B) are weak compared to the Coulomb interaction, use the perturbation theory to calculate the corrections to the energy due to Zeeman splitting and fine structure.
3. Apply the relativistic correction for the momentum of the electron (H_{rel}), as well as the correction due to the Darwinian term (H_{Darwin}).

In a zero order approximation, the electron Hamiltonian in a hydrogen atom consists of operators of kinetic energy and Coulomb interaction:

$$\widehat{H}_0 = -\frac{\hbar^2}{2\mu}\vec{\nabla}^2 - \frac{e^2}{4\pi\epsilon_0 r}, \quad (2)$$

where $\hbar$ is the Planck constant, $\mu = m_e M/(m_e + M)$ – the reduced mass of electron, m_e – the electron mass, M – the nucleus mass, $\vec{\nabla}$ – del operator, e – the electron charge, ϵ_0 – the dielectric constant, $r \equiv |\vec{r}|$ – the module of the electron radius vector. Solving the Pauli equation in the zero approximation, we obtain the energies of states and wave functions:

$$E_0^{(n)} = -\frac{\mu c^2}{2}\frac{\alpha^2}{n^2}, \quad (3)$$

$$|\psi\rangle^{(n,l,m_l,m_s)} \equiv |n, l, m_l, m_s\rangle, \quad (4)$$

where $\alpha = e^2/4\pi\epsilon_0\hbar c$ is the fine structure constant, c – the speed of light. The next step was the application of perturbation theory to take into account the effects of spin-orbit interaction and interaction with the magnetic field:

$$\widehat{H}_{LS} = \frac{1}{2m_e^2 c^2}\frac{e^2}{4\pi\epsilon_0}\frac{1}{r^3}\vec{L}\vec{S}, \quad (5)$$

$$\widehat{H}_B = \frac{\mu_B B}{\hbar}\left(\hat{L}_z + g_s\hat{S}_z\right), \quad (6)$$

where $\vec{L}, \vec{S}$ are the operators of the orbital and spin momenta of the electron, $\hat{L}_z, \hat{S}_z$ – operators of their projections on the direction of the magnetic field, $\mu_B = e\hbar/2m_e$ – the Bohr magneton, B – the magnitude of the magnetic field, g_S – magnetic momentum of the electron. In order to apply the perturbation theory we have to assume that $\langle\widehat{H}_{LS}\rangle \ll \langle\widehat{H}_0\rangle$ and $\langle\widehat{H}_B\rangle \ll \langle\widehat{H}_0\rangle$, which holds true in the case of solar magnetic fields. As a result, we obtain the expressions for the energy and wave

functions of the electron in the hydrogen atom which take into account the magnetic field and fine structure:

$$(H_0 + H_B + H_{LS})\left|\psi\right\rangle^{(n,l,m_j,\pm)} = E_{0,B,LS}^{(n,l,m_j,\pm)}\left|\psi\right\rangle^{(n,l,m_j,\pm)}, \tag{7}$$

$$E_{0,B,LS}^{(n,l,m_j,\pm)} = E_0^{(n)} + \Delta E_{B,LS}^{(n,l,m_j,\pm)}, \tag{8}$$

where m_j – eigenvalue of $\hat{J}_z$: $\hat{J}_z|\psi\rangle = \hbar m_j|\psi\rangle$, «$\pm$» - quantum number, which takes the values of 1 and -1, and which differentiates the states with same n, l and m_j. The energy correction $\Delta E_{B,LS}^{(n,l,m_j,\pm)}$, which accounts for the magnetic field and fine structure, is as follows:

$$\Delta E_{B,LS}^{(n,l=0,m_j,\pm)} = \pm W\beta\frac{g_s}{2}, \tag{9}$$

$$\Delta E_{B,LS}^{(n,l\neq 0,m_j,\pm)} = \begin{cases} W\left[l+\beta\left(l+\frac{g_s}{2}\right)\right], & m_j = l+1/2 \\ \frac{W}{2}\left[2m_j\beta - 1 \pm \sqrt{\beta^2(g_s-1)^2 + 4m_j\beta(g_s-1) + (2l+1)^2}\right], & |m_j| \neq l+1/2 \\ W\left[l-\beta\left(l+\frac{g_s}{2}\right)\right], & m_j = -l-1/2, \end{cases} \tag{10}$$

where $W = m_e c^2\alpha^4/4n^3 l(l+1/2)(l+1)$, $\beta = \mu_B B/W$ – dimensionless magnetic field.

Eigenfunctions $|\psi\rangle^{(n,l,m_j,\pm)}$ for the cases of $l = 0$ and $|m_j| = l + 1/2$ are the eigenfunctions of the unperturbed Hamiltonian. For $l = 0$ we have:

$$|\psi\rangle^{(n,l=0,m_j,\pm)} = |n, l, m_l = 0, m_s = m_j\rangle, \tag{11}$$

and for $|m_j| = l + 1/2$ the eigenfunctions are:

$$|\psi\rangle^{(n,l,m_j=l+1/2,\pm)} = |n, l, m_l = l, m_s = 1/2\rangle \tag{12}$$

$$|\psi\rangle^{(n,l,m_j=-l-1/2,\pm)} = |n, l, m_l = -l, m_s = -1/2\rangle \tag{13}$$

In the case of $|m_j| \neq l + 1/2$ eigenfunctions $|\psi\rangle^{(n,l,m_j,\pm)}$ cannot be written as a single eigenfunction of the unperturbed Hamiltonian. However, since the eigenfunctions $|\psi\rangle^{(n,l,m_l,m_s)}$ form the complete set, we can express any functions in terms of a linear combination of the eigenfunctions $|\psi\rangle^{(n,l,m_l,m_s)}$. It turns out that $|\psi\rangle^{(n,l,m_j,\pm)}$ are linear combinations of only 2 eigenfunctions $|\psi\rangle^{(n,l,m_l,m_s)}$ of the unperturbed Hamiltonian:

$$|\psi\rangle^{(n,l,m_j,\pm)} = \sin\phi\ \ |n, l, m_l = m + 1/2\,, m_s = -1/2\rangle + \\ + \cos\phi\ \ |n, l, m_l = m - 1/2\,, m_s = 1/2\rangle, \tag{14}$$

where the coefficients $\sin\phi$ and $\cos\phi$ depend on the magnetic field magnitude β:

$$\phi = \arctan\frac{\sqrt{4l(l+1)-4m^2+1}}{2m+\beta(g_s-1)\pm\sqrt{\beta^2(g_s-1)^2+4m\beta(g_s-1)+(2l+1)^2}} \tag{15}$$

Finally, we have to account for the relativistic correction to the orbital momentum

$$\Delta E_{rel} = \frac{m_e c^2}{2}\frac{\alpha^4}{n^4}\left(\frac{3}{4} - \frac{n}{l+\frac{1}{2}}\right), \tag{16}$$

and the correction due to the Darwin term:

$$\Delta E_{Darwin} = \frac{m_e c^2}{2}\frac{\alpha^4}{n^3}\delta_{l,0}. \tag{17}$$

Finally, the energy of the electron states in the hydrogen atom in an arbitrary magnetic field is

$$E^{(n,l,m_j,\pm)} = E_0^{(n)} + \Delta E_{B,LS}^{(n,l,m_j,\pm)} + \Delta E_{rel}^{(n,l)} + \Delta E_{Darwin}^{(n,l)}. \quad (18)$$

This result allows us to calculate the splitting of the atomic terms in the magnetic field. In order to obtain the spectral line profiles, we have to calculate the intensities of the transitions between different terms. This means that we have to evaluate the matrix elements of the electromagnetic field operator on the $|\psi\rangle^{(n,l,m_j,\pm)}$ functions. However, since the eigenfunctions $|\psi\rangle^{(n,l,m_j,\pm)}$ can be expressed as a linear combination of the unperturbed functions $|\psi\rangle^{(n,l,m_l,m_s)}$, the matrix elements on $|\psi\rangle^{(n,l,m_j,\pm)}$ are the linear combinations of matrix elements on the $|\psi\rangle^{(n,l,m_l,m_s)}$, which are already studied in details.

The described algorithm allows us to calculate the energies and the intensities of the transitions that form the shape of the observed spectral line (Fig. 3). In order to calculate the shape of the spectral line, we have to make some assumptions regarding the broadening mechanisms of the components that form it. Since typical temperatures in solar flares often reach a million degrees, the main broadening mechanism is thermal. In addition, due to the complex spatial structure of the flares, the shape of the line has to account for the turbulent (non-thermal) velocities and the possibility of the presence of several emission components. Different broadening mechanisms likely have a much weaker influence on the shape of the line profiles.

Thermal broadening and turbulent velocities can be accounted for by representing each spectral line component as a Gaussian profile in such a way that its area is proportional to the component's relative intensity. The width of the Gaussian profile then is determined by the temperature and turbulent velocities:

$$\Delta\lambda_{1/2} = \frac{2\lambda_0}{c}\sqrt{\left(\frac{2kT}{m} + \xi_{turb}^2\right)\ln(2)}, \quad (19)$$

where $\Delta\lambda_{1/2}$ is the FWHM of the profile, λ_0 – wavelength of the spectral line, k – the Boltzmann constant, T – temperature, m – hydrogen atom mass, ξ_{turb} – turbulent velocity.

According to calculations using Allen's Astrophysical Quantities (Cox, 2002), a partial Paschen-Back effect occurs in the Hα line beginning from about B = 10 kG, when more or less close groups of many split subcomponents are formed (Fig. 7). In this case, the overall picture of the line splitting is far from the classical Zeeman triplet, but if this picture is superimposed on the temperature and turbulent expansion with a scale factor of σ = 50 mÅ, then the corresponding picture will be almost indistinguishable from the Zeeman triplet with a total half-width of the united components of about 300 mÅ (Fig. 8).

At a magnetic field B = 100 kG, the full Paschen-Back effect occurs, in which the splitting subcomponents are grouped much more closely than at B = 10 kG (Fig. 9). With the same temperature and turbulent expansion corresponding to σ = 50 mÅ, we have very narrow (~200 mÅ) and strongly split components (Fig. 10). With this in mind, we can admit that the very narrow observed features (~500 mÅ) in Fig. 4 may well be real.

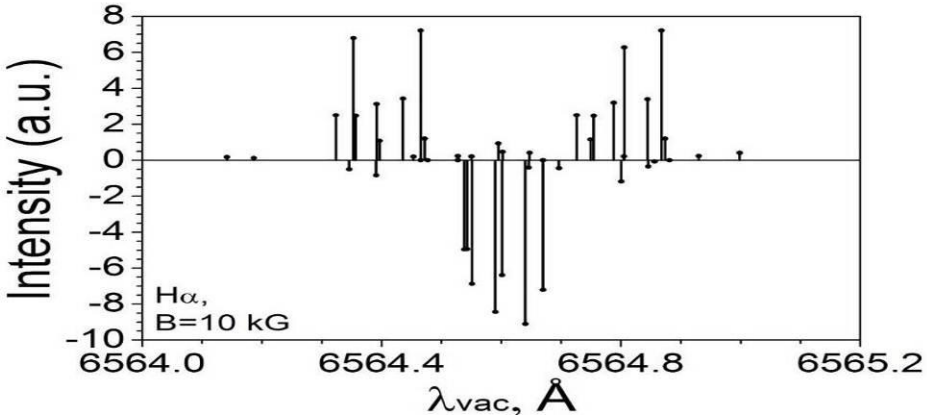

Fig. 7. Fine structure of the Hα line of the hydrogen atom in the magnetic field of 10 kG. The magnetic fields of such order correspond to the partial Paschen-Back effect.

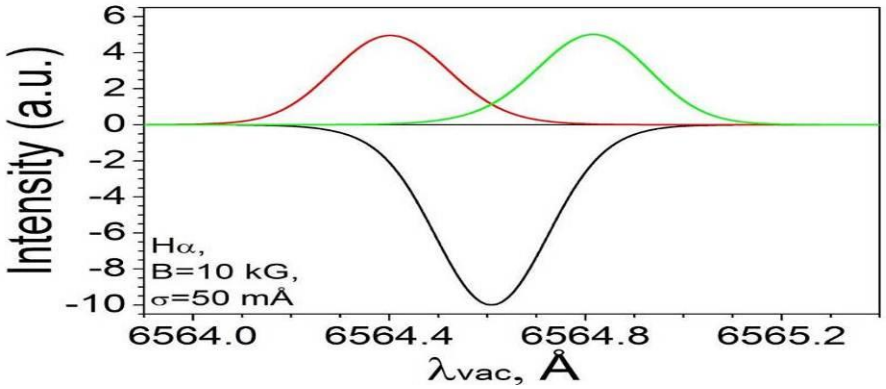

Fig. 8. Hα line profiles in the transverse magnetic field B = 10 kG for Doppler spectral expansion by the temperature and turbulent velocities that correspond to $\sigma = 50$ мÅ.

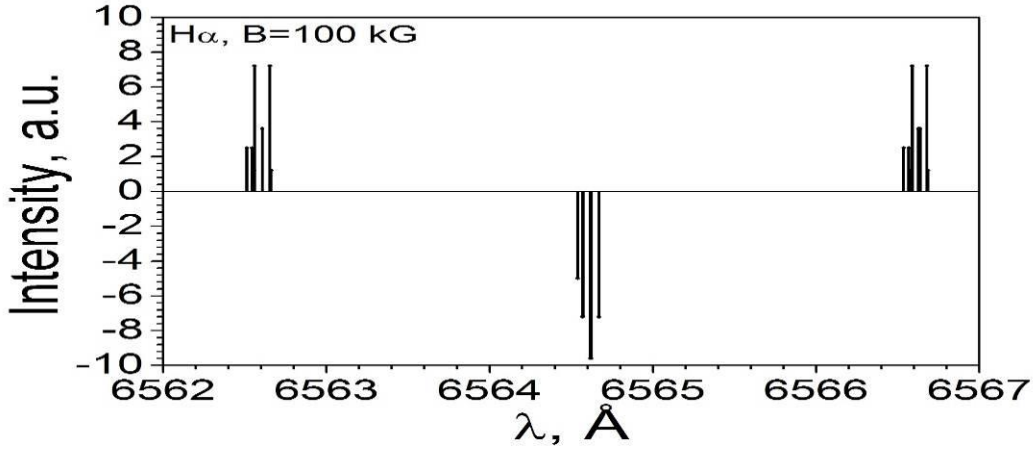

Fig. 9. Fine structure of the Hα line of the hydrogen atom in the magnetic field of 100 kG. The magnetic fields of such order correspond to the full Paschen-Back effect.

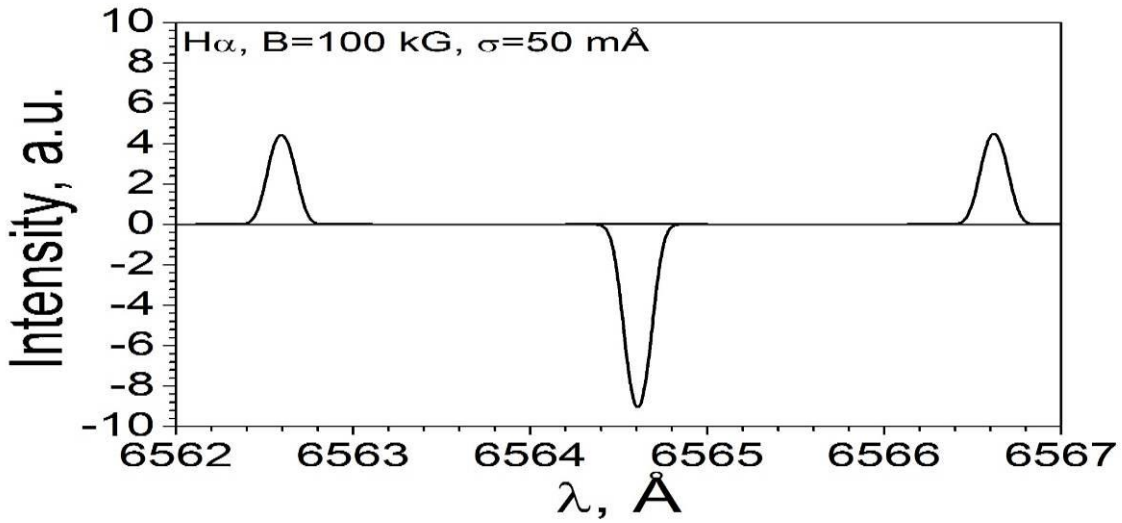

Fig. 10. Hα line profiles in the transverse magnetic field B=100 kG for Doppler spectral expansion by temperature and turbulent velocities that correspond to σ = 50 мÅ.

Another useful conclusion follows from an examination of Fig. 10: the effective Lande factor g_{aff} of the H-alpha line in the case of B = 100 kG is close to 1.00. Recall that this is exactly the value of the Lande factor for a normal Lorentzian triplet. In this case, the well-known formula for linking Zeeman splitting $\Delta\lambda_H$ to magnetic field B can be written as

$$\Delta\lambda_H = 4.67 \times 10^{-13} g_{eff} \lambda_0^2 B = 4.67 \times 10^{-13} \lambda_0^2 B = 2.01 \times 10^{-5} B, \quad (20)$$

where $\Delta\lambda_H$ is in Å, and B – in gauss (G).

If we suppose that splitting of Stokes V peaks placed at $\Delta\lambda \approx \pm$ (1.8-1.9) Å, see Figs. 3 and 4 above, occurred due to the Zeeman effect, then corresponding magnetic fields according to formula (20) are 86-95 kG. Alternative interpretations should be considered before claiming the reality of such fields.

7. Discussion

In purely instrumental terms, the following question may be the most controversial: could the detected effects (Fig. 2-5) be caused by purely instrumental polarization (IP) in observations of the Zeeman effect, and not by solar causes? It should be noted that the issue of the influence of instrumental polarization on such measurements has already been analyzed in detail by the authors in Yakovkin & Lozitsky (2021) and Lozitsky (2016). For magnetic field measurements by $I + V$ and $I - V$ profiles, the essential influence of IP occurs due to the linear-to-circular transformation effect (LCT-effect). If linear polarization is zero, the observed $I + V$ and $I - V$ profiles are not distorted by IP. In this case, we can expect an insignificant role of IP for observations of magnetic features with almost longitudinal field (γ = 0° or 180°). Thus, under the Zeeman effect,

instrumental polarization cannot have a significant effect on the far wings of the line, at a distance from the center $\Delta\lambda$ = 1.5-3.5 Å, where the parameter $dI/d\lambda$ is close to zero.

However, another scenario can be assumed: the observed profiles of the Hα line reflect the Stark effect, not the Zeeman effect, i.e. they reflect strong electric fields in the solar flare region. Depending on the magnitude of the electric field strength and the filling factor, this can give a more or less strong linear polarization, which, being transformed by instrumental polarization, is partially converted into circular polarization and modulated by the polarization analyzer. It is important that under the Stark effect and observations across the electric field in the spectrum, two types of components must be linearly polarized: *p* components with a plane of polarization parallel to the electric field vector and *s* components whose plane of polarization is perpendicular to the field strength vector (Frish, 2010). Since the *p* and *s* components must also have a certain mutual splitting (shift) along the wavelengths, the transformation of this polarization into a circular due to inclined reflections from the telescope and spectrograph mirrors may, in principle, lead to the spectral effects similar to those noted above. If the observations are made along the electric vector, *p* components do not appear, and *s* components must be unpolarized. As a result, under the Stark effect, such effects can be recorded with a circular polarization analyzer only when there is instrumental polarization and the line of sight forms an angle of about 90° with the electric field vector.

Calculations show that at electric fields E = 4000 V / m observed by Chen et al (2020) in the region of X point of a solar flare leads to a too weak splitting of the Hα line due to the Stark effect, ~ 10^{-2} Å, which is 2 orders of magnitude less than required to explain the polarization we observed. Wider spectral effects are possible at high electron concentrations in solar flares, ~ 10^{10} cm^{-3}, but they occur in lines of high numbers of Balmer series and, in addition, such effects should not give polarization in the line profile (see, eg, Kurochka & Maslenikova, 1970). As for the existence of much stronger regular electric fields (E >> 4000 V / m), this can be considered currently only hypothetical, not yet conclusively proven. Spectral manifestations symmetrical with respect to the center of the line and having opposite circular polarization also testify in favor of the Zeeman effect (Fig. 3-5). When the Hα line is split due to the Stark effect, *p* and *s* splitting components should give a more chaotic picture (Frish, 2010). That is why we are inclined to the point of view that the recorded spectral manifestations are really due to the Zeeman effect caused by a superstrong magnetic field. It is very interesting that the value of 10^5 G is in agreement with the magnetic field at the bottom of the convective zone (Fan, 2004).

8. Conclusion

Our study confirms the hypothesis of Bruce (1966) that the magnetic field strength in solar flares can reach ~ 100 kG. This hypothesis, based on spectral observations in unpolarized light (Stokes parameter I), is confirmed in our work based on the analysis of Stokes V profiles. We found reliable polarization at a distance of $\Delta\lambda \approx \pm$ (1.8-1.9) Å from the center of the Hα line, which changes its sign when passing through the center of the line and has a symmetrical appearance relative to this center (Fig. 3). That is why we believe that these are most probably the manifestations of the Zeeman effect, corresponding to very strong magnetic fields, ~ 90 kG. With such giant fields, the full Paschen-Back effect should theoretically be observed in the H-alpha line,

when the observed cleavage components should be combined into very close groups with an apparent half-width of about 0.2 Å. Indeed, the observed *V* profiles contain relatively narrow features that have a visible half-width of about 0.5 Å (Fig. 4). Similar effects were not found in the active solar protuberance of July 24, 1999, with a fairly wide emission in Hα (~5 Å), which may indicate that such giant fields are a relatively rare phenomenon in the solar atmosphere.

Acknowledgements

The authors are grateful to unknown reviewers for useful notes and critical comments. This study was funded by the Taras Shevchenko National University of Kyiv, project No. 22БФ023-03.

References

Anfinogentov S.A., Stupishin A.G., Mysh'akov I.I., Fleishman G.D., 2019. Record-breaking coronal magnetic field in solar active region 12673. The Astrophys. J. Lett. 880, article id. L29, 5 pp.

Bethe H.A., Salpeter E.E., 1957. Quantum mechanics of one- and two-electron systems. In: Atoms I / Atome I. Encyclopedia of Physics / Handbuch der Physik, vol 7 / 35. Springer, Berlin, Heidelberg. https://doi.org/10.1007/978-3-642-45869-9_2.

Blom A., 2005. Exact solution of the Zeeman effect in single-electron systems. Physica Scripta, T120, 90–98. doi:10.1088/0031-8949/2005/t120/014.

Bogod V.M., Stupishin A.G., Yasnov L.V., 2012. On magnetic fields of active regions at coronal heights. Solar Phys. 276, 61-73.

Brosius J.W., White S.M., 2006. Radio measurements of the height of strong coronal magnetic fields above sunspots at the solar limb. Astrophys. J. 641, L69–L72.

Bruce C.E.R., 1966. Magnetic fields in solar flares. Observatory. 86, 82.

Centeno R., 2018. On the weak field approximation for Ca 8542 Å. The Astrophys. J. 866, article id. 89, 14 pp.

Chen B., Shen C., Gary D.E. Reeves K.K. et al., 2020. Measurement of magnetic field and relativistic electrons along a solar flare current sheet**.** Nature Astronomy**.** 4, 1140-1147**.**

Cox A. N., 2002. Allen's Astrophysical Quantities. doi:10.1007/978-1-4612-1186-0.

Fan Yu., 2004. Magnetic fields in the solar convection zone. Living Rev. in Solar Phys.1, Iss. 1, article id. 1, 74 pp.

Fleishman G.D., Gary D.E., Chen B., Kuroda N., Yu S., Nita G.M., 2020. Decay of the coronal magnetic field can release sufficient energy to power a solar flare. Science. 367, 278-280.

Frish S.E., 2010, Optical atom spectra. St.-Peterburg. Moscow. Krasnodar, 656 p.

Garcia, H. A. 1994. Temperature and emission measure from GOES soft X-ray measurements. Solar Phys. 154, 275-308.

Garcia, H. A., McIntosh, P. S. 1992. High-temperature flares observed in broadband soft X-rays. Solar Phys. 141, 109-126.

Gary D.E., Chen B., Dennis B.R., Fleishman G.D. et al., 2018. Microwave and hard X-ray observations of the 2017 September 10 solar limb flare. The Astrophys. J. 863, article id. 83, 9 pp.

Kirichek E.A., Solov'ev A.A., Lozitskaya N.I., Lozitskii V.G., 2013. Magnetic fields in a limb flare on July 19, 2012. Geomagn. and Aeronomy. 53, 831–834.

Kleint L., 2017. First detection of chromospheric magnetic field changes during an X1-Flare. Astrophys. J. 834, art. id. 26, 10 pp.

Koval A.N., 1977. On the measurement of magnetic fields in prominences and flares by the photographic method. Bull. of the Crimean Astrophys. Obs. 57, 133–143.

Koza J., Kuridze D., Heinzel P. et al. 2019. Spectral diagnostics of cool flare loops observed by the SST. I. Inversion of the Ca II 8542 Å and Hβ lines. The Astrophys. J. 885, article id. 154, 13 pp.

Kramida, A. E., 2010. A critical compilation of experimental data on spectral lines and energy levels of hydrogen, deuterium, and tritium. Atomic Data and Nuclear Data Tables, 96(6), 586–644. doi:10.1016/j.adt.2010.05.001.

Kuckein C., Centeno R., Martínez Pillet V. et al. 2009. Magnetic field strength of active region filaments. Astron. Astrophys. 501, 1113-1121.

Kuckein C., Gonzalez Manrique S.J., Klient L., Asenio Ramos A. 2020. Determining the dynamics and magnetic fields in He I 10830 Å during a solar filament eruption. Astron. Astrophys. 640, id.A71, 12 pp.

Kuridze D., Mathioudakis M., Morgan H., Oliver R. et al., 2019. Mapping the magnetic field of flare coronal loops. Astrophys. J. 874, art. id. 126, 12 pp.

Kurochka L.N., Maslenikova L.B., 1970. The electron concentration determination by the limitly admitted lines. Solar Phys. 11, 33-41.

Landi Degl'Innocenti E.L., 1982. On the effective Landé factor of magnetic lines. Solar Physics. 77, No. 1-2, 285-289.

Libbrecht T., de la Cruz Rodriguez J., Danilovic S., Leenaarts J. et al., 2019. Chromospheric condensations and magnetic field in a C3.6-class flare studied via He I D_3 spectro-polarimetry. Astron. Astrophys. 621, id.A35, 21 pp.

Lozitsky V.G., 1980. On the calibration of magnetograph measurements taking into account the spatially unresolved inhomogeneties. Physica Solariterris, Potsdam. 14, 88-94.

Lozitsky V.G., 1993. Superstrong magnetic fields in the solar atmosphere. Kinematics and Physics of Celestial Bodies. 9, 18-25.

Lozitsky V.G., 1998. Observations of magnetic fields with strengths of several tesla in solar flares. Kinematics and Physics of Celestial Bodies. 14, 307-316.

Lozitsky V.G., 2009. Observational evidences to the 10^5 G magnetic fields in active regions on the Sun. Journal of Physical Studies. 13(2), 2903-1-2903-8.

Lozitsky V.G., 2015. Small-scale magnetic field diagnostics in solar flares using bisectors of $I \pm V$ profiles. Adv. Space Res. 55, 958–967.

Lozitsky V.G., 2016. Indications of 8-kilogauss magnetic field existence in the sunspot umbra. Adv. Space Res. 57, 398–407.

Lozitsky V.G., Statsenko M.M., 2006, Proc. of 3rd Int. Scient. Semin. "Physics of the Sun and stars", Elista, Kalmyk Univ., 29 May-2 June 2006, 43–50.

Lozitsky V.G., Staude J., 2008. Observational evidences for multi-component magnetic field structure in solar flares. J. Astrophys. Astron. 29, 387–404.

Lozitsky, V.G., 2011. Observational evidences for extremely strong magnetic fields in solar flares. Int. J. Astron. Astrophys. 1 (3), 147–154.

Sasikumar Raja K., Venkata Suresh, Singh Jagdev B. Raghavendra Prasad, 2022. Solar Coronal Magnetic Fields and Sensitivity Requirements for Spectropolarimetry Channel of VELC Onboard Aditya-L1. Adv. Space Res. 69, 814-822. DOI: 10.1016/j.asr.2021.10.053

Schad T.A., Penn M.J., Lin H., Judge P.G., 2016. Vector magnetic field measurements along a cooled stereo-imaged coronal loop. The Astrophys. J. 833, article id. 5, 16 pp.

Tomozov V.M., 1990. Turbulent stark effect: Possible observational manifestations in solar flares. Journal of Quantitative Spectroscopy and Radiative Transfer. 44, 171-175.

Unno W., 1956. Line formation of a normal Zeeman triplet. Publs. Astron. Soc. Japan. 8, 108–125.

Wei Yudian , Chen Bin, Yu Sijie, Wang Haimin, Jing Ju, and Gary Dale E., 2021. Coronal Magnetic Field Measurements along a Partially Erupting Filament in a Solar Flare. The Astrophys. J., 923:213 (11pp). https://doi.org/10.3847/1538-4357/ac2f99.

Xu, Z., Lagg, A., Solanki, S. and Liu, Y., 2012. Magnetic fields of an active region filament from full stokes analysis of Si I 1082.7 nm and He I 1083.0 nm. The Astrophys. J. 749(2), 138 (11pp).

Yadav R., Baso C.J.D., da la Cruz Rodríguez J., Calvo F., 2020. Stratification of physical parameters in a C-class solar flare using multi-line observations. eprint arXiv:2011.02953.

Yakovkin I.I., Veronig A.M., Lozitsky V.G., 2021. Magnetic field measurements in a limb solar flare by hydrogen, helium and ionized calcium lines. Adv. Space Res. 68, 1507-1518.

Zemanek E.N., Stefanov A.P., 1976. Splitting of some spectral lines of FeI in magnetic field. Vestnik Kiev University, Seria Astronomii. 18, 20-36.